

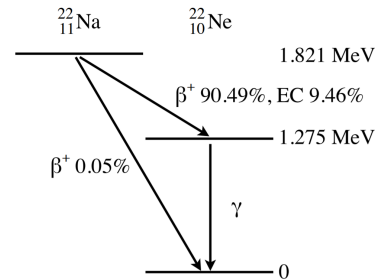
# Gamma Ray Spectroscopy & Beta Particles in a Magnetic Field

Natan Szczepaniak

8th November 2018

This set of experiments looks at the different aspects of  $\beta^-$  and  $\beta^+$  decay in common radioactive isotopes including Na-22, Cs-137, Co-60 and Sr-90. Two different energy spectroscopy methods are demonstrated and used to draw conclusion about the interaction of gamma rays with matter and beta particles with magnetic fields.

## 1 Theory



Following the decay schemes of common radioactive isotopes including Na-22, Co-60, Cs-137, Am-241 and Sr-90 we will explore the nature of beta decay using two different spectroscopic methods. We will examine the interaction between gamma rays and matter by looking at the different attenuation coefficients of different materials and kinetic energies comparing our values to ones found in literature. The spectra of radioactive sources will also be used to visualise and explain the effects of phenomena such as Compton Scattering and Internal conversion. Additionally, the behaviour of both  $\beta^+$  and  $\beta^-$  particles under a magnetic field of variable strength will be used to find an energy spectrum letting us find the kinetic energies available for the decays. In the following experiments we will look at beta decay schemes which result in the emission of  $\beta$  particles and gamma rays due to the isotopes being unstable. Using Sodium-22 we can demonstrate this well with the use of a decay diagram as followed.

As we see, the Na-22 isotope decays emitting a positron ( $\beta^+$ ) and producing a daughter isotope Ne-22 which then emits a 1.275 MeV  $\gamma$  ray which should be seen as a peak on the energy spectrum given by a scintillator. Interestingly, some of the positrons also annihilate with electrons creating additional  $\gamma$  rays which would correspond to another visible peak. In addition to this, the spectrum exhibits features caused by phenomena such as back-scattering and internal conversion which will both be explored in the following experiments. The diagram also demonstrates two  $\beta^+$  particles of energies 546keV and 2.274MeV being emitted however the abundance of 546keV  $\beta^+$  particles (90.49%) is much greater so we would expect the peak to be significantly larger than the 2.274MeV. Moreover, we expect that the peaks obtained will not exactly correspond to the ones displayed by the decay schemes as there is a coulomb

interaction between the emitted beta particle and the nucleus that our investigation does not account for. We will use a scintillator counter connected to a computer to detect the gamma ray energy peaks of the given radioactive isotopes, however the scintillator crystal does not detect the beta particles meaning we need another method. As all  $\beta$  particles have a charge associated with them, when in a magnetic field, they experience a force perpendicular to the direction of travel. On this premise, we can send them through a variable uniform magnetic measuring the count rate at a point for each interval and find the desired deflection. As the field strength required for a specific deflection depends on the kinetic energy of the particle, we can use this to obtain an energy spectrum of the particles using equation:

$$Q = \sqrt{(qBrc)^2 + m_0^2c^4} - m_0c^2 \quad (1)$$

For each kinetic energy we find the corresponding count rate to form a spectrum

## 2 Method

### 2.1 Gamma Ray Spectroscopy

Before conducting the experiment, we exposed the device to the emitter of the highest energy gamma rays (Cobalt-60) and adjusted the voltage supplied to the scintillator to cover the whole spectrum of energies we were investigating. Next, we replaced the radioactive source with Sodium-22 calibrated the different energies to the different output channels of the device using the 511keV and 1275keV peaks. With the equipment calibrated, we obtained the energy spectra of Cobalt-60, Sodium-22 and the Caesium-137 mixture by suspending the source above the scintillator and measuring the number of counts (intensity) of each energy. We analysed the spectra using the computer program by generating a gaussian of equal width at each of the peaks which gave us the energy at the center of the peak and the associated sigma value which we used to judge the degree of accuracy of our results. Lastly we compared these obtained values to the ones available in the decay schemes to validate our results. Next, we investigated the linear

attenuation coefficient of aluminium for the different energy peaks we found by placing an absorber on a Perspex cylinder atop the scintillator counter and varied its thickness to observe differences in the intensity (In our case we measured the count rate however these two are proportional). We also made sure to measure the background count rate with no source present and take that away from the obtained results to make sure the attenuation coefficient solely depends on the radiation from the source.

$$I = I_0 \exp(-\mu x) \quad (2)$$

Measuring the intensity of the radiation as a function of thickness we obtained the linear attenuation coefficient  $\mu$  by rearranging the above equation to:

$$\ln(\frac{I}{I_0}) = -\mu x \quad (3)$$

We then plotted a graph of  $\ln(\frac{I}{I_0})$  against  $x$  for each of the results where the gradient was simply equal to the linear attenuation coefficient of gamma rays in the material. We checked our obtained results against the literature and calculated the half value depth  $d_{\frac{1}{2}}$  using the equation.

$$d_{\frac{1}{2}} = \frac{\ln(2)}{\mu} \quad (4)$$

to draw further conclusions. Due to the high count rate of the mixed nuclide sample containing Cs-137 and Am-241 (which gave us a smooth spectrum) we used it to explore the features of the Compton effect in the spectrum and find out if the 59.5keV energy peak is caused by internal conversion. To make the features more prominent on the graph we fit a polynomial function to the background radiation and took it away from the spectrum obtained. Before looking the graph, we calculated the maximum and minimum energy of the scattered gamma photon using the Compton scattering equation. The maximum energy of the scattered photon would occur at a scattering angle of  $0^\circ$  and the minimum would be observed if the scattering angle is  $180^\circ$  (back-scattering). This would result in a characteristic shape on our spectrum with two small, but distinct peaks with a continuum in between. When an excited state loses its

energy by ejecting an atomic electron from the center of the atom next to the nucleus, electrons drop down to the vacant states emitting x-rays, this is known as internal conversion. To see if this phenomenon is present we accurately measured the energy of the K-line peak in the lower energy region and compared it to literature to see if the peak is in fact caused by this effect.

## 2.2 Beta Particles in Magnetic Fields

To find the energy spectrum of the beta particles emitted by our two radioactive isotopes (Na-22 and Sr-90) we used a beta spectroscope consisting of a Geiger-Mueller tube connected to a counter, an electromagnet connected to a power supply of a variable current and a hall probe contained in a non-magnetisable circular container with three holes for the GM-tube, hall probe and sample.

Before introducing the radioactive source to the beta spectroscope, we made sure that we knew the magnetic field strengths for the corresponding currents by measuring the magnetic field with the hall probe in the current range of -2 amps to 2 amps. We made sure that the hall probe was giving us the correct measurements by orientating it the right way giving us positive magnetic field strength readings for positive currents. This is important as the magnetic field direction needed to be reversed between measurements of  $\beta^-$  particles in Sr-90 and  $\beta^+$  particles in Na-22) as differently charged particles behave differently in a uniform magnetic field.

Once calibrated, we tested the two radioactive sources by measuring the count rate as a function of the magnetic field three times for each source and taking an average taking away the background radiation. We then converted the magnetic field strengths to the kinetic energies of the particles using Equation 1 allowing us to plot the two *beta* spectra. We then compared the values of total available kinetic energy  $Q_0$  on our spectrum to the total available kinetic energy of the decay shown in the decay scheme. Additionally, as we tested both  $\beta^+$  and  $\beta^-$  we compared the behaviour of the two particles revealing their interaction with the nucleus.

## 3 Results

### 3.1 Gamma Ray Spectroscopy

For all of the spectra we observed, the background radiation we observed was distributed mostly in the lower energy end of the spectra in a continuous distribution which we attributed to the Bremsstrahlung (Breaking) radiation. This is present because we are investigating charged particles which are accelerated by the nucleus of the parent element. For the Cobalt-

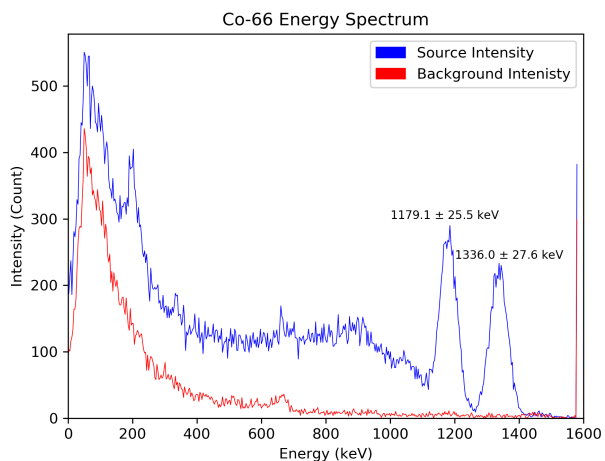
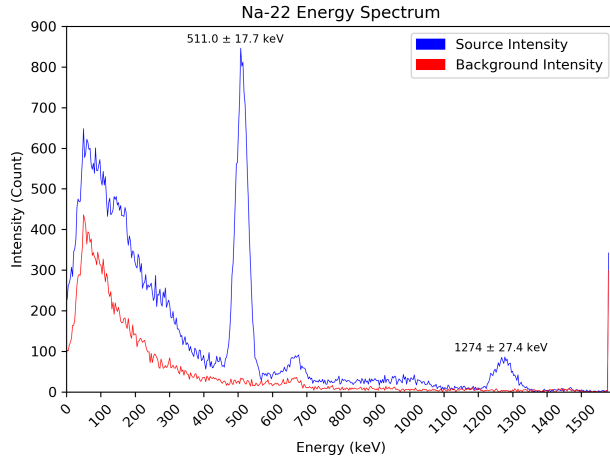


Figure 1: Energy Spectrum of Cobalt-60

60 Figure 1 spectrum we observed 2 distinct peaks at  $1179.1 \pm 25.5 \text{ keV}$  and  $1336.0 \pm 27.6 \text{ keV}$  by fitting a Gaussian to the peaks. It can be clearly seen that these two gamma rays correspond to the two characteristic gamma rays produced by the change in energy level of Co-60 daughter element Ni-60. The excited states of this daughter element are short lived meaning the two rays are emitted virtually simultaneously however we can see from the intensity that the intensity of the  $1336 \text{ keV}$  peak is slightly lower than that of predeceasing energy peak as one is dependent on the other in the decay scheme. Our uncertainty was rather high but our values were accurate meaning there was random error in our result which could have been avoided by taking the measurements over a longer period of time.



**Figure 2:** Energy Spectrum of Sodium-22

As expected the Sodium-22 Figure 2 sample produced two peaks, one sharp  $511.0 \pm 17.7$  keV peak and a smaller one at  $1275.0 \pm 27.4$  keV. There is no doubt that the 511.0 keV peak is caused by positron annihilation and the fact that the intensity is so great suggests that the annihilation happens instantly which supports the theory that this is caused by this effect. This sample was used to calibrate the device which is why the values observed correspond to the theoretical values exactly. The uncertainty in these results comes from the fact that the peak is a distribution of energies as the values vary due to other physical phenomena.

The mixed nuclide including Cs-137 and Am-241 (Figure 3) was the most active source we tested giving us much higher counts for the same period of time (5 minutes) making the background radiation much less problematic. We managed to measure  $672.0 \pm 19.9$  keV for the peak corresponding to the daughter element of Cs-137 (Barium-137) dropping to its ground state. Our result lays  $0.5\sigma$  from the actual value of  $662$  keV. As the uncertainty is reasonably low, but the value obtained deviates greatly, this must be the result of a systematic error which in this case may have been caused by the calibration being inaccurate. We concluded that the  $36.7 \pm 12.3$  keV peak is caused by the internal conversion as it resem-

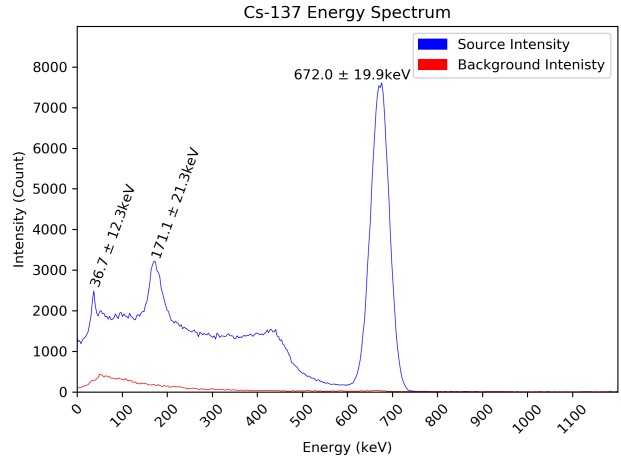


**Figure 3:** Energy Spectrum of Caesium-137

bles a K line in the X-ray energy range over the breaking radiation. This value however does not coincide with the actual value (59.5 keV) and is  $1.85\sigma$  from our experimental result further proving that there must be a systematic error caused by the calibration of the spectrum. These peaks however, follow a general pattern of a Cs-137 spectrum meaning we should be able to use the intensity of the peaks to find the attenuation coefficients for the different energies.

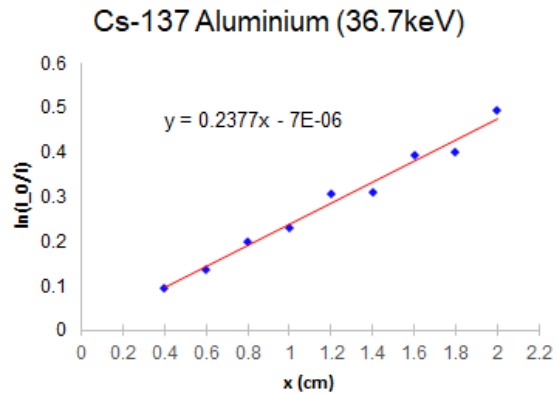


**Figure 4:** Attenuation Graph of 36.7keV Peak

Using the method we mentioned previously, using

a plot of  $\ln(I_0/I)$  against the thickness ( $x$ ) of the absorber, we get out a gradient of  $\mu_E = 0.240 \pm 0.029\text{cm}^{-1}$  (where the uncertainty is the uncertainty in the gradient) for the linear absorption coefficient of aluminum for the of the 36.7 keV peak. This when compared to the actual value of  $\mu_A = 0.51\text{cm}^{-1}$  (for the 59.7 keV peak) is within the right order of magnitude however it is out by a factor of 2. The uncertainty in the gradient is also reasonably high at 15% however the wrong value cannot be attributed to random error as the uncertainty is not big enough for the experimental value reach the actual value. This lower attenuation coefficient is caused by the energy of the peak being uncertain from the previous experiment and perhaps may not be the same energy peak meaning the error in the energy of the peak is not just caused by calibration but the source itself demonstrating properties due to impurities in the Am-241 sample.

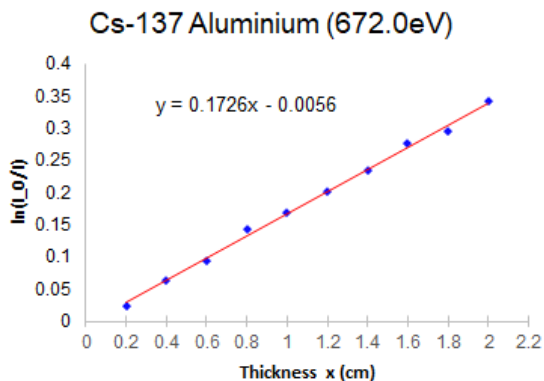


**Figure 5:** Attenuation Graph of 672keV Peak

The result shown in Figure 5 is relatively accurate compared to our previous result giving us a value of  $\mu_E = 0.173 \pm 0.003\text{cm}^{-1}$  which is even closer to the actual value of  $\mu_A = 0.16\text{cm}^{-1}$  (of peak 662keV). The uncertainty in the gradient this time is merely 1.7% meaning we are getting precise results however our experimental value is still quite far from the actual value, once again showing us there is a systematic error in our data however this time it is much lower which corresponds to the lower difference between

our energy peak (667keV) and the theoretical one (662keV) which suggests that this is a key factor in the error we are getting in our results. Lastly, for the attenuation energy of aluminum for 1253keV we measured the 1173.0 keV peak of Co-60 at different thicknesses of the absorber which resulted us in getting the value of  $\mu_E = 0.192 \pm 0.009\text{cm}^{-1}$  which deviated from the actual value further proving a systematic error. The half value depth values were (36.7keV)  $d_{\frac{1}{2}} = 2.88\text{cm}$ , (672keV)  $d_{\frac{1}{2}} = 4.00\text{cm}$ , (1173keV)  $d_{\frac{1}{2}} = 3.61\text{cm}$ . Which generally follows the trend of the higher the energy the lower the penetration depth.

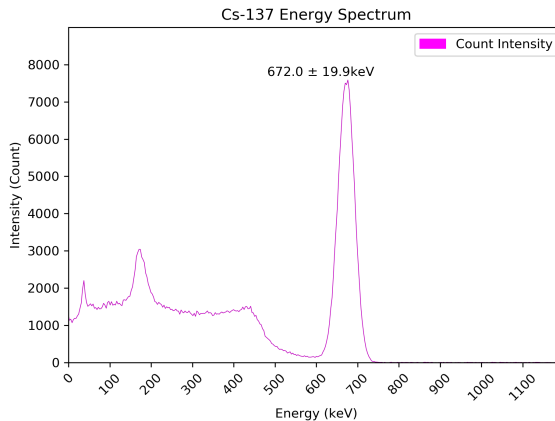


**Figure 6:** Energy Spectrum of Mixed Nuclide

As demonstrated by Figure 6 (Figure 3 with background intensity taken away), the Compton spectrum mentioned previously, is clearly seen in the 200keV and 430keV energy range. The calculated value of the minimum energy of scattered photons using the Compton scattering formula is  $E_{min} = 250\text{keV}$ . As we can see from Figure 3, the back scattering peak was measured to be  $117 \pm 21.3\text{keV}$ . Considering we have encountered systematic errors with this spectrum due to the incorrect calibration, we can say that that the  $117\text{keV}$  peak corresponds to the back scattering effect caused by the Compton effect where photons are reflected with minimum energy. This coupled with the presence of a Compton edge at  $439.6\text{keV}$  gives us strong evidence of the presence of

the Compton effect. Although the internal conversion peak which should be present at 59.5 keV according to decay schemes found in the literature is located at 37.6 keV on our spectrum, it strongly resembles a K line inside the bremsstrahlung X-ray energy region. It is a sharp peak suggesting there is little variation in the energy which would be true for a stream of X-ray photons being emitted due to an electron being "knocked out" of a low energy level.

### 3.2 Beta particle spectroscopy

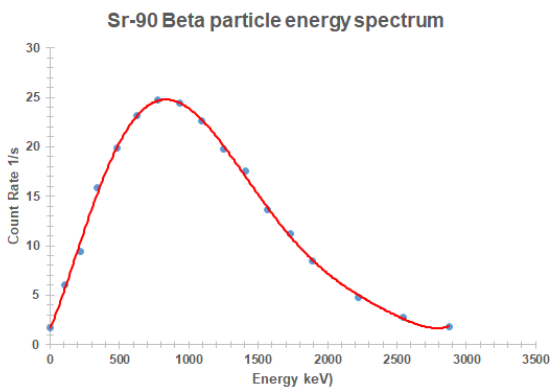


Figure 7: Energy spectrum of beta decay of Sr-90

As seen in Figure 7, the beta particle creates a Gaussian distribution of energies with a  $Q_0$  that we determined to be around 2546.8 keV by drawing a horizontal line from the y intercept and finding where it meets the curve. This is lower than the value of 2274 keV given by the decay scheme. Surprisingly, this is the result we expected because as mentioned previously in the Theory section, Coulomb forces between the particles cause a shift in energy. In the case of  $\beta^{-1}$  decay, the beta particles are attracted back to the nucleus reducing their kinetic energy therefore shifting the spectrum to the left which we observe here. Additionally, the decay scheme outlines that there are more  $\beta^{-}$  particles emitted in the decay scheme suggesting we should see two peaks however we only see one. This is due to the fact that 99.98% of  $\beta^{-}$  particles have the total kinetic energy of 2274

keV.

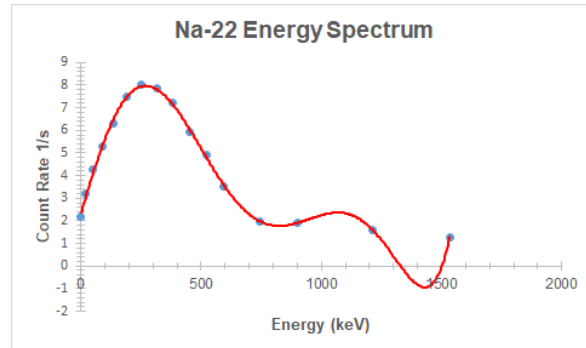


Figure 8: Energy spectrum of beta decay of Na-22

As for Figure 8 which demonstrates the spectrum of energies of  $\beta^{+}$  decay of Na-22 we see much more background noise, contributing to the graph. This is due to the count rate of Sodium-22 being much lower than that of Sr-90 which means the background rate has a much more significant effect on the results. Additionally, there is extra background noise caused by the 511 keV annihilation radiation which further upsets the results meaning the entire spectrum is shifted up despite having accounted for the background radiation. This time, we determined the total kinetic energy available for decay  $Q_0$  to be 745.1 keV which is higher than the theoretical 546 keV. This, once again, is caused by the Coulomb force between the emitted beta particle and the nucleus however this time, the force is repulsive giving the positron more kinetic energy which shows up as an energy spectrum which is shifted to the right. The second peak visible on the spectrum has no physical meaning and is an artifact of fitting a polynomial function to the data with significant background radiation. Lastly, although the values follow the theory the values themselves are not entirely accurate because if this data was to be used to find the extra kinetic energy gained or lost due to the Coulomb forces, that value would not be exact due to the poor measurement method of the data. A different way of finding a more accurate value would be to make a spectrum over a larger range of energies, fit a polynomial function to it and find the values of x (Energy) at the

minimum which would allow for uncertainties to be found.

## 4 Conclusions

In this set of experiments we found the main behaviours governing beta decay in common radioactive isotopes. Despite getting the correct patterns of peaks similar to the ones found in literature, we did not manage to fully demonstrate the correct values for energies of gamma rays. This skewed our results for the rest of the gamma ray experiment and led us to inaccurate values for the linear attenuation coefficient. Although, there must have either been an error in the calibration of the equipment or a problem with the source itself, the value of  $\mu$  of aluminum for the 672 keV we obtained was closest to the real value, there was a mistake in measuring the peaks accurately. Upon reflection, Am-241 did not seem to be present in the mixed nuclide sample we tested and the 36.7 keV peak was a feature of the Cs-137 spectrum whereas the 59.5keV peak was not featured in our data. The attenuation coefficient would still be valid if accounted for the calibration error visible in the 672.0 keV peak. Lastly, for the determination of the beta particle energy spectrum, a better method could have been implemented if the investigation required a certain degree of accuracy to draw conclusions or determine  $Q_0$ .

## References

- Book01 *Gamma Ray Spectroscopy Manuscript*,  
University of Exeter
- [0] [1] *Beta Particles in Magnetic Fields Manuscript*,  
University of Exeter
- [2] *A Study on the Gamma-Ray Attenuation Coefficients of Al<sub>2</sub>O<sub>3</sub> and Al<sub>2</sub>O<sub>3</sub>.TiO<sub>2</sub> Compounds*,  
Journal of Natural and Applied Sciences Volume 22, Special Issue, 312-318, 2018